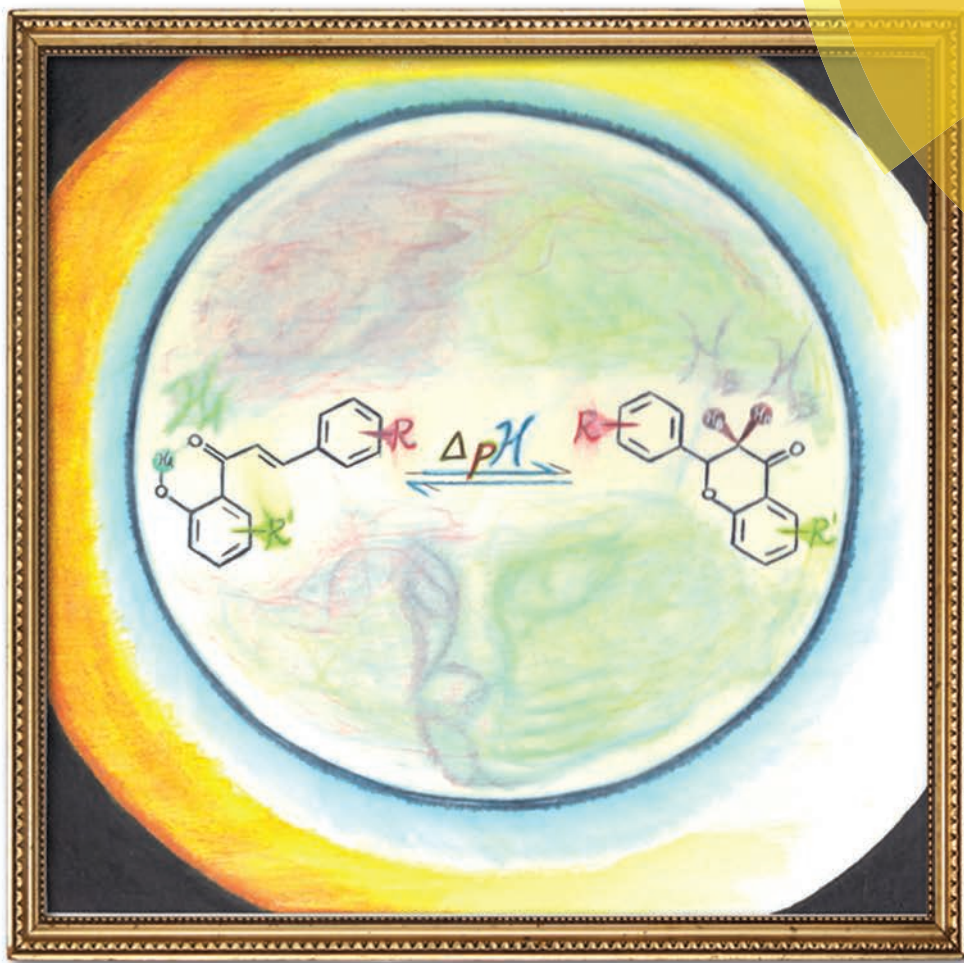


Organic & Biomolecular Chemistry

www.rsc.org/obc



ISSN 1477-0520



PAPER

Marc J. Adler *et al.*

Impact of mono- and disubstitution on the colorimetric dynamic covalent switching chalcone/flavanone scaffold

Impact of mono- and disubstitution on the colorimetric dynamic covalent switching chalcone/flavanone scaffold†

Cite this: *Org. Biomol. Chem.*, 2014, **12**, 5108

Brian M. Muller, Jesse Mai, Reid A. Yocum and Marc J. Adler*

Received 20th February 2014,

Accepted 28th April 2014

DOI: 10.1039/c4ob00398e

www.rsc.org/obc

The effect of aryl substitution on various aspects of the interconversion of *ortho*-hydroxychalcones and flavanones has been studied using multiple spectroscopic techniques. Derivatization of the core scaffold predictably alters the midpoint pH of this equilibration process suggesting its viability for application as a functional colorimetric molecular switch.

Introduction

Molecules that are capable of being reversibly biased towards one of two or more states in response to an external stimulus are called molecular switches.¹ These molecules have not only garnered interest from a fundamental standpoint, but have also found application in a variety of realms^{2–4} including sensing,^{5–8} chemical biology,^{9–12} and functional materials.¹³

The development of scaffolds that can function as molecular switches has been a ripe area of research over the past decade. Approaches include photoswitchable^{14–23} (e.g. azobenzenes, diarylethenes, and spiropyrans) and chemoswitchable molecules^{5–8,13,24,25} (e.g. diphenylacetylene- and hydrazone-based switches), each offering distinct advantages and disadvantages. While photoinitiated switches involve covalent changes taking place to the structure, conformational states in chemoresponsive switches to this point have been stabilized exclusively by weaker non-covalent interactions, rendering these switches less rigidly binary. Despite the robustness of their conformational states, light-responsive molecules offer obvious challenges outside of a well-regulated laboratory environment. To the authors' best knowledge, no chemoswitching scaffold has been developed that relies on the interconversion of covalently differentiated states with opposing conformations.

With these ideas in mind, we sought to develop a novel molecular switch that would incorporate the controllability of chemoresponsive molecules with the rigidity of covalently

differentiated states: a dynamic covalent chemoswitch.²⁶ Ideally, we also desired a system that could be characterized colorimetrically; such an attribute would allow for several distinct advantages including the ability to detect changes (a) at low concentration and (b) on a rapid timescale and (c) the option to utilize a variety of (non-deuterated) solvents.

We identified *ortho*-hydroxychalcone (**1a**) and its readily accessible constitutional isomer flavanone (**2a**) as a potential scaffold for development of such a switch (Fig. 1).²⁷ This system is capable of interconversion in aqueous solutions by altering the pH; the range of pH within which rapid equilibration takes place is ~10 (where flavanone is the only observed isomer) to ~13 (where anionic chalcone is adopted exclusively).²⁸ Subsequent acidification provides a kinetically stable solution of either isomer. While **1a** is held in conformation by a tight hydrogen bond between H_A and the carbonyl oxygen, **2a** is rigidified by the newly formed covalent bond.

The interconversion of these classes of molecules has been studied in the context of understanding how this process occurs in nature,^{29–33} but prior to our initial disclosure the

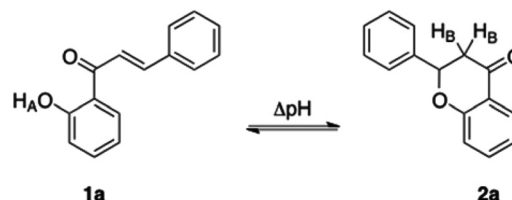


Fig. 1 Isomerism between *ortho*-hydroxychalcone (**1a**) and flavanone (**2a**) can be reversibly controlled by altering solution pH. These two constitutional isomers rapidly interconvert between pH 10 and 13, with flavanone (**2a**) the only species present at the low end of this range and anionic chalcone (**1a**) observed exclusively in more alkaline solutions. This change can be detected colorimetrically, as only **1a** absorbs strongly in the ultraviolet region.

Department of Chemistry & Biochemistry, Northern Illinois University, 1425 W Lincoln Hwy, DeKalb, IL 60115, USA. E-mail: mjadler@niu.edu; Tel: +1 815 753 9236

† Electronic supplementary information (ESI) available: Synthetic procedures, characterization data (¹H and ¹³C NMR, IR, and HRMS), sigmoidal curves derived from UV/Vis equilibration assay, rate determination assay plots, and procedure and plots for DMSO titration studies. See DOI: 10.1039/c4ob00398e

scaffold had not been explored for the applied purpose of functioning as a molecular switch. Interestingly, another chalcone-based scaffold has been used as a switch: 2-hydroxychalcones are known to interconvert with anthocyanins.¹ This construct, while elegant and useful, lacks the structural rigidity and binary nature (imparted by the hydrogen bond between the 2'-hydroxy and the carbonyl) we sought for our dynamic covalent chemoswitch.

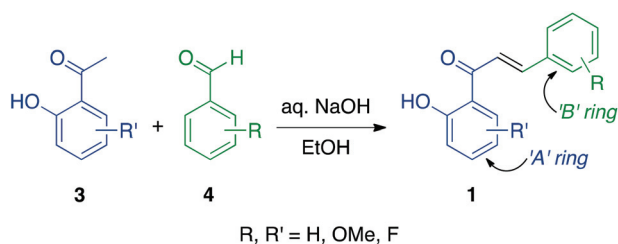
Previously,²⁷ we established and detailed a UV/Vis spectrophotometric assay for investigation of this isomerism and subsequently analyzed the impact of a single methoxy substituent in a variety of positions. Chalcones were placed in solutions of varying pH (8.5–13) and allowed to reach equilibrium with the flavanone isomer. For each compound, there exists a pH at which the solution contains a 1 : 1 ratio of chalcone to flavanone; the impact of substitution on the switching scaffold was measured by tracking the shift of the midpoint pH of the equilibrium: the putative equivalence point. Demonstrating this ability to be structurally tuned was a crucial step in the development of the scaffold as a functional molecular switch.

These preliminary findings indicated that the effect of substitution on the dynamic interconversion is complex. While previous studies have focused on the reliance of this putative equivalence point exclusively on the pK_a of H_A , the data indicated that this was not the case; we proposed that the pK_a of H_B also plays a role in this dynamic process (Fig. 1).

In order to further probe the utility of this scaffold as a molecular switch and its susceptibility to electronic bias, we were interested in expanding this study to include a substituent of a different identity (namely, fluorine) and also to see if the effects of multiple substitutions would be linear or synergistic. Additionally, we sought to gain deeper insight into the influence of aromatic substituent electronics on the isomerization process by investigating not only the thermodynamics of isomerization but also the kinetics.

Results and discussion

The synthesis of the molecules to be evaluated was performed in a similar manner to the procedure previously disclosed (Scheme 1). A high-throughput synthetic route was developed for the conversion of acetophenones and benzaldehydes to chalcone products; in this manner, sufficient material was generated for all described studies.



Scheme 1 General synthesis of substituted chalcone derivatives (1).

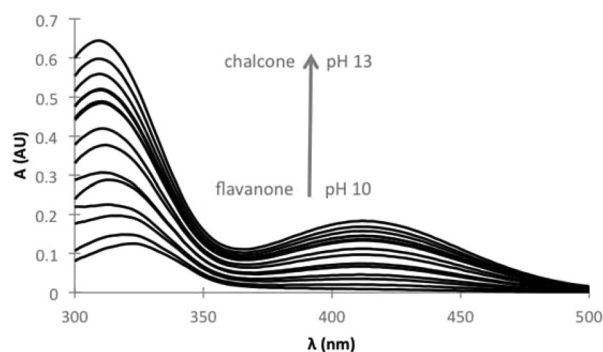


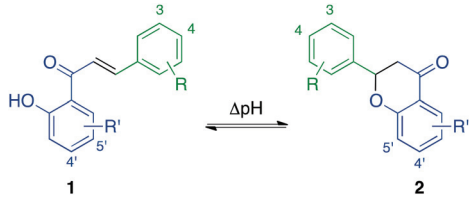
Fig. 2 Raw UV/Vis absorbance data for the conversion of *ortho*-hydroxychalcone **1a** to flavanone **2a**.

UV/Vis studies on midpoint pH

The pH-dependent constitutional isomerization was studied using the previously described UV/Vis spectrophotometric assay. The interconversion was tracked by absorbance at the λ_{max} of the highly conjugated chalcones (Fig. 2); this value was more significantly affected by substitution on the 'B' ring and ranged from 304 to 340 nm (Table 1). While in some cases overlap of the absorbance spectra of the two species was observed in this region, signal amplification ($A_{[chalcone]}/A_{[flavanone]}$) in each case was sufficient for quantitative monitoring.

The putative equivalence point (*i.e.* the pH at which there exists a 1 : 1 ratio of the two isomers) was obtained by fitting the pH-dependent absorbance data with a sigmoidal curve (Fig. 3). While the scope of this study only included two monosubstituted molecules at each of the explored positions, it is instructive to consider the data from a linear free energy relationship (between midpoint pH and substitution) perspective. The construct chosen for this analysis was the Swain–Lupton equation,³⁴ which separates the effects of each substituent to field (F) and resonance (R) effects.^{35–37} This dataset seemed appropriate as an analytical tool for this system as discerning the relevant classical Hammett parameters (*e.g.* σ , σ^+ , σ^-) is difficult in this case.

Swain–Lupton substituent constants (F , R) with more positive values indicate more significant electron withdrawing effects and those with negative values of greater magnitude representing an increasing ability to donate electron density. Relevant to this study are the values for fluoro ($F = 0.45$, $R = -0.39$) and methoxy ($F = 0.29$, $R = -0.56$) substituents; in both cases the substituents are inductively withdrawing and resonantly donating. Position-dependent reaction constants f and r (Table 2) were derived from the midpoint pH shift data for the studied monosubstituted compounds (Table 1, entries 2–6, 11, 16, and 21). Compounds **1b–1e** feature a single substituent on the 'B' ring. This data emphatically shows that substitution on the 4 position is more influential than at the 3 position (Table 2, entry 2); in fact, substitution at the 3 position seems to have little effect on this equilibrium. While the difference in consequences between the respective substitutions could be expected from a resonance standpoint, the contrast in force

Table 1 Key results of studies on the switching *ortho*-hydroxychalcone (1)/flavanone (2) derivatives


Entry	Compounds	R	R'	λ_{\max}^a (nm)	ΔpH^b	Rate, 1 to 2 ^c	Rate, 2 to 1 ^d	δ, H_A^e (ppm)	$\Delta\delta, \text{H}_A^e$ (ppm mL ⁻¹ d ₆ -DMSO)
1	1a/2a	H	H	310	0	1	1	12.8	-1.45
2	1b/2b	4-OMe	H	338	-0.36	0.7	0.6	12.92	-1.81
3	1c/2c	3-OMe	H	306	+0.05	1.1	1.0	12.78	-1.68
4	1d/2d	4-F	H	312	-0.15	1.0	1.5	12.75	-1.74
5	1e/2e	3-F	H	306	+0.04	0.9	1.0	12.7	-1.76
6	1f/2f	H	4'-OMe	314	-0.10	0.2	0.5	13.41	-1.72
7	1g/2g	4-OMe	4'-OMe	336	-0.31	0.6	0.6	13.52	—
8	1h/2h	3-OMe	4'-OMe	312	-0.14	0.8	0.3	13.4	—
9	1i/2i	4-F	4'-OMe	314	-0.30	0.1	0.5	13.39	—
10	1j/2j	3-F	4'-OMe	310	-0.10	0.1	0.6	13.32	—
11	1k/2k	H	5'-OMe	309	+0.42	1.7	0.9	12.35	-1.83
12	1l/2l	4-OMe	5'-OMe	340	+0.02	1.3	1.6	12.46	—
13	1m/2m	3-OMe	5'-OMe	306	+0.45	1.7	0.5	12.32	—
14	1n/2n	4-F	5'-OMe	310	+0.45	2.0	0.4	12.31	—
15	1o/2o	3-F	5'-OMe	306	+0.55	0.7	0.4	12.26	—
16	1p/2p	H	4'-F	310	-0.95	0.4	2.0	13.18	-1.59
17	1q/2q	4-OMe	4'-F	336	—	—	1.7	13.31	—
18	1r/2r	3-OMe	4'-F	306	-0.94	1.4	1.7	13.17	—
19	1s/2s	4-F	4'-F	312	-1.18	0.5	0.3	13.15	—
20	1t/2t	3-F	4'-F	306	-1.10	0.2	2.3	13.08	—
21	1u/2u	H	5'-F	310	-0.24	1.6	4.0	12.51	-1.65
22	1v/2v	4-OMe	5'-F	340	-0.50	2.1	2.1	12.63	—
23	1w/2w	3-OMe	5'-F	304	-0.15	1.8	1.3	12.5	—
24	1x/2x	4-F	5'-F	314	-0.22	0.2	2.5	12.47	—
25	1y/2y	3-F	5'-F	306	-0.1	0.2	1.3	12.42	—

^a λ_{\max} reported is for chalcones (1), at which conversion was monitored for all UV/Vis experiments. ^b ΔpH relative to midpoint pH of 1a/2a (11.46). ^c Rates for conversion of 1 to 2 relative to $k_{(1a \rightarrow 2a)}$ (0.002576 s⁻¹). ^d Rates for conversion of 2 to 1 relative to $k_{(2a \rightarrow 1a)}$ (0.1911 s⁻¹). ^e δ from ¹H NMR spectra of chalcones (1) taken in CDCl₃. ^f Datapoint unable to be acquired.

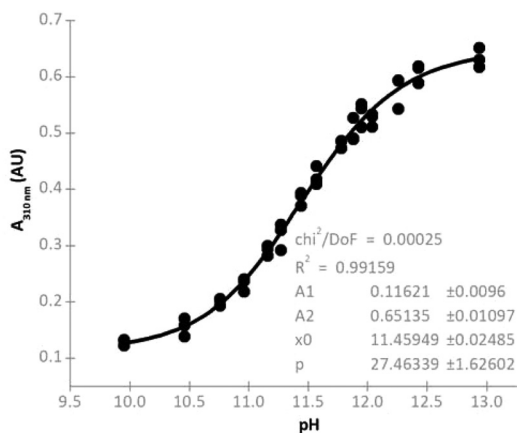


Fig. 3 pH vs. absorbance plot for unsubstituted parent compounds 1a/2a, assembled from data seen in Fig. 2.

effects is somewhat surprising considering that this effect is ostensibly correlated to proximity. Substitution at the 4 position (Table 2, entry 1) is positively correlated with *F* and *R*; this indicates that the midpoint pH increases as electron

Table 2 Swain–Lupton position-dependent reaction constants derived from ΔpH of monosubstituted switching derivatives

Entry	Substituent position	<i>f</i>	<i>r</i>	% <i>r</i>
1	4-	0.4	0.85	68
2	3-	0.02	-0.08	n/a
3	4'-	-3.55	-1.66	32
4	5'-	-2.15	-1.86	46

density is withdrawn from this position. Additionally, a %*r* of 68 demonstrates the significant resonance contribution of substituents at this location on this interconversion.

Much larger values of the Swain–Lupton position-dependent reaction constants are obtained when evaluating the substitution of the 'A' ring. Substitution at either the 4' (Table 2, entry 3) or 5' (Table 2, entry 4) position shows negative correlation to both force and resonance effects; this result demonstrates that the midpoint pH decreases with the inclusion of electron withdrawing substituents on the 'A' ring.

Confidence in these Swain–Lupton parameters may be gained from the equilibrium data collected for the disubstituted

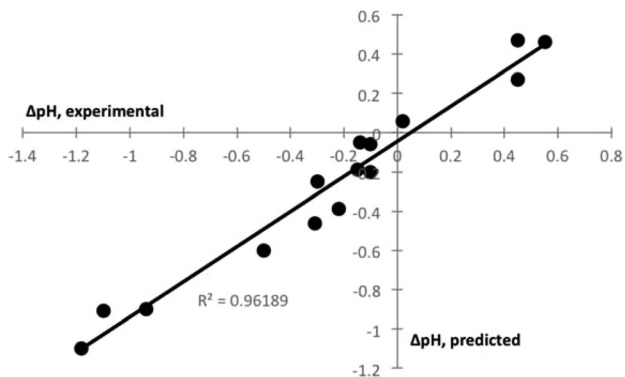


Fig. 4 Experimental vs. predicted ΔpH for disubstituted derivatives. Experimental ΔpH was derived for each compound by subtracting the midpoint pH for each derivative from the midpoint pH for **1a/2a**. For each disubstituted compound, this value was plotted against the ΔpH expected from adding the ΔpH for each of the two substituents individually. This treatment reveals a strong linear correlation between midpoint pH and substitution.

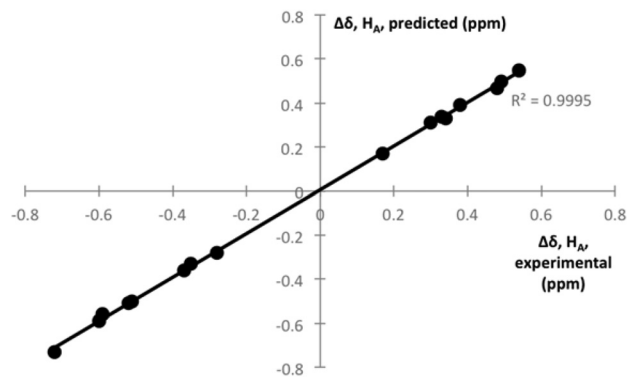


Fig. 5 Experimental vs. predicted ^1H NMR chemical shift (δ) of H_A . Experimental $\Delta\delta$ was obtained by subtracting the δ for each derivative from the δ for **1a**. For each disubstituted compound, this value was plotted against the $\Delta\delta$ expected from adding the $\Delta\delta$ of each of the two substituents individually. This plot reveals a strong linear correlation between δ of H_A and substitution.

compounds. If the data were linearly related, it would be expected that the effect of each substitution on the midpoint pH of the chalcone/flavanone interconversion would be additive. This correlation is observed: the midpoint pH of the disubstituted compounds has a strong correlation to the values predicted by adding the effects of individual substituents on the putative equivalence point (Fig. 4).

Certain aspects of the derived Swain–Lupton constants f and r appear at odds with the prevalent idea that the putative equivalence point of this equilibrium is entirely dependent on the $\text{p}K_\text{a}$ of the phenolic proton (H_A). In general, electron-withdrawing substituents at any position would be expected to lower this $\text{p}K_\text{a}$ value consequently lowering the midpoint pH of the isomerism. Experimentally, while electron withdrawal from the 'A' ring does correspond to this expectation, the opposite effect is observed for substitution of the 'B' ring.

The $\%r$ is indeed greater at the 5' position than at the 4' position, which would be expected when assessing the impact on the H_A . This value, however, does not approach that to be expected from a simple reaction manifold with a single substituent in a position to interact in a resonant manner with the group of interest (80% r). Interestingly, this change in $\%r$ is largely due not to a change in the resonance contribution (r), but rather to the varying impact of the force constant (f).

^1H NMR studies

The dependence of midpoint pH on H_A $\text{p}K_\text{a}$ can be further probed using NMR spectroscopy. While the $\text{p}K_\text{a}$ of alcoholic protons cannot be directly correlated to the chemical shift in the ^1H NMR, the collected data shows that substitution has a predictable impact on the chemical shift of the phenolic proton (Fig. 5). However, no direct significant linear relationship exists between this chemical shift and midpoint pH (Fig. 6). This shows that while substitution does correlate to the electronic environment of this proton, this relationship is not analogously correspondent to the effect on midpoint pH.

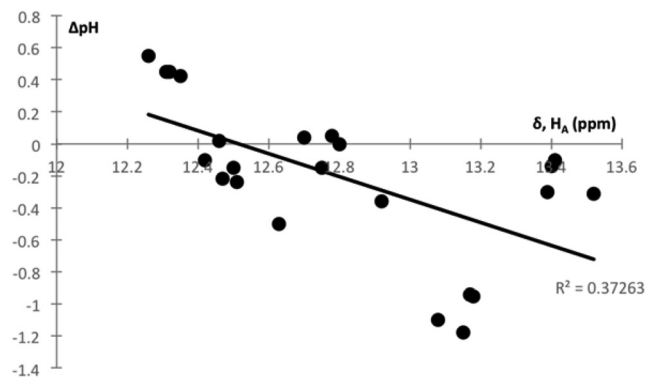
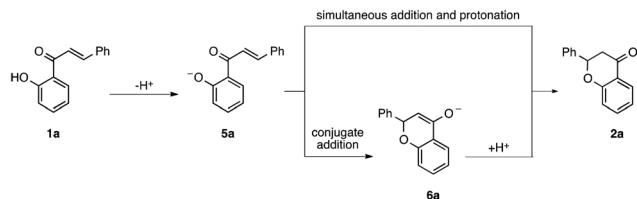


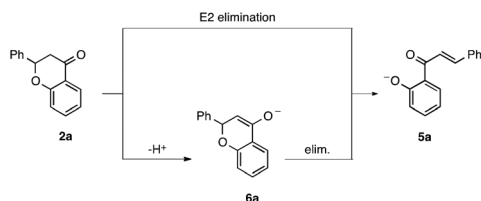
Fig. 6 Chemical shift (δ) of H_A vs. midpoint pH. This plot shows that despite the linear dependence of each of these variables independently to substitution, there is no significant correlation between them.

The chemical shifts of these protons, however, are also affected by the presence of a strong intramolecular hydrogen bond between this phenolic proton and the carbonyl oxygen. A DMSO titration study was performed to query the impact of substitution on hydrogen bond strength. The results established no significant consistent variance amongst the hydrogen bond strengths in the examined mono-substituted derivatives (Table 1) and this suggests that the chemical shift of H_A for a given compound is not affected by this factor.

We have previously postulated that while the $\text{p}K_\text{a}$ of H_A is an important factor in chalcone/flavanone interconversion the $\text{p}K_\text{a}$ of H_B is also significant. The precise mechanisms for interconversion in both directions (Schemes 2 and 3) have been previously debated,^{29–33} and specific commentary on this process is beyond the scope of this study. It is clear, however, that H_B is directly involved in the transformation of flavanone to chalcone, and that this process could have significant influence on the equilibrium of these two constitutional isomers. Our hypothesis is that lowering the $\text{p}K_\text{a}$ of H_B would facilitate



Scheme 2 Possible mechanisms for chalcone (**1a**) to flavanone (**2a**) at pH 9.25.



Scheme 3 Possible mechanisms for flavanone (**2a**) to chalconate (**5a**) at pH 13.

the conversion of flavanone to chalcone, thus having an analogous effect to H_A and lowering the midpoint pH.

From this perspective, the similar r value for substitution at 4' and 5' makes more sense, as resonance with either the phenol or the carbonyl can impact this overall equilibrium in the same direction, *i.e.* electron withdrawal will lower the midpoint pH. This may also help to explain the counterintuitive findings with regard to 'B' ring substitution: lack of molecular rigidity (additionally precluding interaction with H_B through a π system)³⁸ renders the Swain–Lupton treatment complex to apply.

UV/Vis studies on relative rates

In an effort to further explore the individual contribution of the pK_a s of H_A and H_B to the equilibrium, the rates of both unidirectional reactions were studied. Relative rate constants for the quantitative conversion of **1** to **2** and **2** to **1** were obtained by monitoring the UV/Vis absorbance of these reactions under non-equilibrating conditions (Table 1). Importantly, the complete conversion of both starting materials to their respective products was verified by isolation and NMR characterization of **1a** and **2a** after kinetic measurement acquisition.

Substitution on the 'B' ring exclusively (Table 1, entries 2–5) generally did not have a large effect on the rate in either direction. Notably, the inclusion of a methoxy substituent at the 4 position slowed conversion in both directions, while incorporation of a fluoro substituent at the same location only affected the flavanone to chalcone rate and in fact sped up this reaction.

Derivatives bearing a single substituent on the 'A' ring only, however, displayed marked rate differences. Substitution at the 4' position (Table 1, entries 6 and 16) slowed the conversion of chalcone to flavanone but displayed diametrically opposed activity with respect to the reverse reaction. In the 5' position

(Table 1, entries 11 and 21), while both substituents mildly enhanced the rate of isomerization from chalcone to flavanone, only the fluoro group had a significant impact in the other direction. This variance in impact suggests that different factors are determining the rate in each direction, again conflicting with the presumption that pK_a of H_A is the sole mediator of the interconversion.

Investigation of disubstituted derivatives revealed that the linear free energy relationship between substitution and the studied equilibrium surprisingly did not extend to the kinetics of the reaction in either direction (**1** to **2** or **2** to **1**): there is no statistical correlation between the rates predicted by multiplying the effects of the individual substituents and the actual rates for the disubstituted compounds (Fig. 7 and 8). The non-linearity of this data highlights the mechanistic complexity of the studied interconversion and suggests either a change in mechanism or at the very least a change in the rate-determining step. Sifting through the myriad factors at play and derivation of meaningful data from these results are both beyond

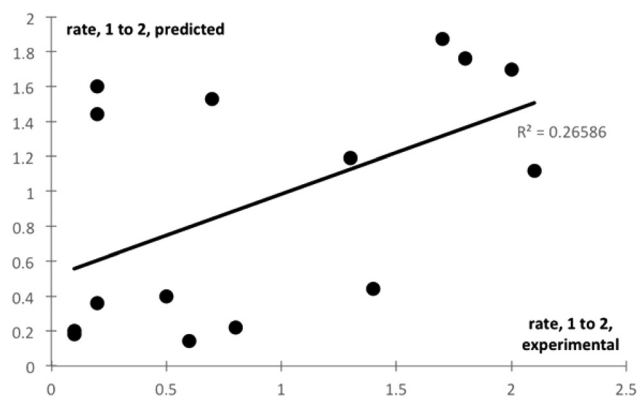


Fig. 7 Plot of predicted vs. experimental relative rates for the quantitative conversion of chalcones (**1**) to flavanones (**2**) at pH 9.25. This demonstrates the non-linear effect of substitution on rate of conversion in this direction.

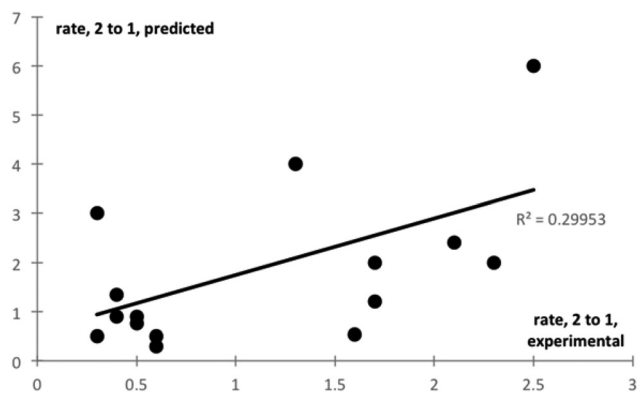


Fig. 8 Plot of predicted vs. experimental relative rates for the quantitative conversion of flavanones (**2**) to chalcones (**1**) at pH 13. This demonstrates the non-linear effect of substitution on rate of conversion in this direction.

the scope of the current work, however it is further evidence against the prevailing notion that there is a sole factor (*i.e.* pK_a of H_A or, similarly, stability of chalconate 5) mediating interconversion.

Conclusions

This work has elucidated several interesting substituent-dependent features of the reversible interconversion of *ortho*-hydroxychalcones and flavanones. It has been shown that the putative equivalence point – the pH at which a solution contains a 1 : 1 mixture of isomers – can be altered electronically by substitution of either of the aromatic moieties. Analogues featuring mono-fluorination of the 'B' ring (**1d/2d**, **1e/2e**) show similar activity to the previously described mono-methoxylated structures (**1b/2b**, **1c/2c**), while derivatives bearing a fluorine on the 'A' ring (**1p/2p**, **1u/2u**) exhibit significantly altered switching properties when compared to their methyl ether counterparts (**1f/2f**, **1k/2k**). Of particular interest is the **1p/2p** equilibrium, which displayed the greatest midpoint pH shift of all of the investigated mono-substituted derivatives.

A linear free energy relationship between substituents and midpoint pH can be described by and understood through use of the Swain–Lupton equation. This relationship cannot be extended to the kinetics of the forward and reverse reactions independently; the mechanistic complexity of this equilibrating scaffold is evident in this finding. The Swain–Lupton data coupled with the lack of correlation between the midpoint pH and either (a) H_A 1H NMR chemical shift (despite the linear substituent-dependence of this data) and (b) the hydrogen bond strength indicates that the shift in midpoint pH is not due solely to the pK_a of H_A . These findings contribute to our understanding of this scaffold and will aid in the development of structural derivatives for use as dynamic covalent molecular switches.

Selected experimental procedures

Procedure for UV/Vis equilibration assay to determine midpoint pH

A 4×10^{-4} M stock solution of chalcone (**1**) in ethanol was prepared. Into a cuvette was added 150 μ L of chalcone solution followed by 1.85 mL of aqueous buffer by way of autopipette. Each sample was prepared in triplicate and all samples were equilibrated in a fridge at 2.6 °C for 2 hours. The samples were removed and stored at ambient temperature for 1 hour. The UV-Vis spectrum was taken from 290–500 nm for each sample. The absorbance at λ_{max} for each pH was then plotted in Origin and fitted using a logistic sigmoidal function iteratively until χ^2 was minimized, with x_0 representing the midpoint.

Procedure for UV/Vis assay to determine chalcone to flavanone rates

A 4×10^{-4} M stock solution of chalcone (**1**) in ethanol was prepared. Into a cuvette was added 150 μ L of this solution

followed by 1.85 mL of 9.25 pH $NaHCO_3$ buffer. Immediately following the addition of buffer, absorbance at the chalcone's λ_{max} was measured every 5 seconds for 9000 seconds. A plot of $\ln[A/A_0]$ vs. time was fitted linearly; the slope of this line was used to determine the relative rate.

Procedure for UV/Vis assay to determine flavanone to chalcone rates

A 4×10^{-4} M stock solution of flavanone (**2**) in ethanol was prepared. Into a cuvette was added 150 μ L of this solution followed by 1.85 mL of 12.75 pH KCl buffer. Immediately following the addition of buffer, absorbance at the corresponding chalcone's λ_{max} was measured every 0.2 seconds for 240 seconds. A plot of $\ln[A/A_0]$ vs. time was fitted linearly; the slope of this line was used to determine the relative rate.

Acknowledgements

Funding graciously provided by Northern Illinois University. The authors thank Dr Heike Hofstetter (NIU) for spectroscopic assistance and Prof. Louise Charkoudian (Haverford College) for helpful discussions.

Notes and references

- B. L. Feringa and W. R. Browne, *Molecular Switches*, Wiley-VCH, Weinheim, 2nd edn, 2011 and references contained therein.
- L. Fabbrizzi and A. Poggi, *Chem. Soc. Rev.*, 1995, **24**, 197–202.
- H. Sugimoto, T. Kimura and S. Inoue, *J. Am. Chem. Soc.*, 1999, **121**, 2325–2326.
- W. A. Velema, W. Szymanski and B. L. Feringa, *J. Am. Chem. Soc.*, 2014, **136**(6), 2178–2191.
- I. M. Jones and A. D. Hamilton, *Org. Lett.*, 2010, **12**, 3651–3653.
- I. M. Jones and A. D. Hamilton, *Angew. Chem., Int. Ed.*, 2011, **50**, 4597–4600.
- I. M. Jones, H. Lingard and A. D. Hamilton, *Angew. Chem., Int. Ed.*, 2011, **50**, 12569–12571.
- X. Su and I. Aprahamian, *Chem. Soc. Rev.*, 2014, **43**, 1963–1981.
- A. A. Beharry and G. A. Woolley, *Chem. Soc. Rev.*, 2011, **40**, 4422–4437.
- T. Fehrentz, M. Schönberger and D. Trauner, *Angew. Chem., Int. Ed.*, 2011, **50**, 12156–12182.
- W. Szymański, J. M. Beierle, H. A. V. Kistemaker, W. A. Velema and B. L. Feringa, *Chem. Rev.*, 2013, **113**, 6114–6178.
- M. A. Kienzler, A. Reiner, E. Trautman, S. Yoo, D. Trauner and E. Y. Isacoff, *J. Am. Chem. Soc.*, 2013, **135**, 17683–17686.
- X. Su, S. Voskian, R. P. Hughes and I. Aprahamian, *Angew. Chem., Int. Ed.*, 2013, **52**, 10734–10739.

- 14 K. Matsuda and M. Irie, *J. Photochem. Photobiol., C*, 2004, **5**, 169–182.
- 15 B. L. Feringa, *J. Org. Chem.*, 2007, **72**, 6635–6652.
- 16 I. Thanopoulos, P. Kral, M. Shapiro and E. Paspalakis, *J. Mod. Opt.*, 2009, **56**, 686–703.
- 17 M. R. Banghart, A. Mourrot, D. L. Fortin, J. Z. Yao, R. H. Kramer and D. Trauner, *Angew. Chem., Int. Ed.*, 2009, **48**, 9097–9101.
- 18 A. A. Beharry, O. Sadovski and G. A. Woolley, *J. Am. Chem. Soc.*, 2011, **133**, 19684–19687.
- 19 M. Natali and S. Giordani, *Chem. Soc. Rev.*, 2012, **41**, 4010–4029.
- 20 J. García-Amorós and D. Velasco, *Beilstein J. Org. Chem.*, 2012, **8**, 1003–1017.
- 21 D. Bléger, J. Schwarz, A. M. Brouwer and S. Hecht, *J. Am. Chem. Soc.*, 2012, **134**, 20597–20600.
- 22 H. M. D. Bandara and S. C. Burdette, *Chem. Soc. Rev.*, 2012, **41**, 1809–1825.
- 23 P. Stawski, M. Sumser and D. Trauner, *Angew. Chem., Int. Ed.*, 2012, **51**, 5748–5751.
- 24 Y. Sohtome, T. Yamaguchi, S. Tanaka and K. Nagasawa, *Org. Biomol. Chem.*, 2013, **11**, 2780–2786.
- 25 S. Grunder, P. L. McGrier, A. C. Whalley, M. M. Boyle, C. Stern and J. F. Stoddart, *J. Am. Chem. Soc.*, 2013, **135**, 17691–17694.
- 26 S. J. Rowan, S. J. Cantrill, G. R. L. Cousins, J. K. M. Sanders and J. F. Stoddart, *Angew. Chem., Int. Ed.*, 2002, **41**, 898–952.
- 27 J. Mai, E. Hoxha, C. E. Morton, B. M. Muller and M. J. Adler, *Org. Biomol. Chem.*, 2013, **11**, 3421–3423.
- 28 A. Cisak and C. Mielczarek, *J. Chem. Soc., Perkin Trans. 2*, 1992, 1603–1607.
- 29 K. B. Old and L. Main, *J. Chem. Soc., Perkin Trans. 2*, 1982, 1309–1312.
- 30 J. J. P. Furlong and N. S. Nudelman, *J. Chem. Soc., Perkin Trans. 2*, 1988, 1213–1217.
- 31 C. O. Miles and L. Main, *J. Chem. Soc., Perkin Trans. 2*, 1988, 195–198.
- 32 N. S. Nudelman and J. J. P. Furlong, *J. Phys. Org. Chem.*, 1991, **4**, 263–270.
- 33 R. G. Button and P. J. Taylor, *J. Chem. Soc., Perkin Trans. 2*, 1992, 1571–1580.
- 34 Swain–Lupton equation: $\sigma\rho = fF + rR$.
- 35 C. G. Swain and E. C. Lupton, *J. Am. Chem. Soc.*, 1968, **90**, 4328–4337.
- 36 S. G. Williams and F. E. Norrington, *J. Am. Chem. Soc.*, 1976, **98**, 508–516.
- 37 C. G. Swain, S. H. Unger, N. R. Rosenquist and M. S. Swain, *J. Am. Chem. Soc.*, 1983, **105**, 492–502.
- 38 P. W. Peterson, N. Shevchenko and I. V. Alabugin, *Org. Lett.*, 2013, **15**, 2238–2241.